

Generation of functional liver tissue by establishing hepatobiliary connections ex vivo

Naoki Tanimizu (✉ tanimizu@sapmed.ac.jp)

Sapporo Medical University <https://orcid.org/0000-0001-8167-1401>

Norihisa Ichinohe

Sapporo Medical University

Yasushi Sasaki

Sapporo Medical University <https://orcid.org/0000-0002-3500-8059>

Tohru Itoh

Institute for Quantitative Biosciences, The University of Tokyo <https://orcid.org/0000-0002-6579-1638>

Ryo Sudo

Keio University

Tomoko Yamaguchi

National Cancer Centre

Takashi Katsuda

University of Pennsylvania

Takashi Tokino

Sapporo Medical University

Takahiro Ochiya

Tokyo Medical University

Atsushi Miyajima

Institute of Molecular and Cellular Biosciences, University of Tokyo

Toshihiro Mitaka

Sapporo Medical University

Article

Keywords: liver tissue, hepatocytes, cytotoxic bile, hepatobiliary connections

Posted Date: November 3rd, 2020

DOI: <https://doi.org/10.21203/rs.3.rs-96037/v1>

License:   This work is licensed under a Creative Commons Attribution 4.0 International License.

[Read Full License](#)

Abstract

In the liver, the bile canaliculi of hepatocytes are connected to intrahepatic bile ducts lined with cholangiocytes, which remove cytotoxic bile from the liver tissue. We have developed a hepatobiliary organoid using mouse hepatocyte progenitors and cholangiocytes. Hepatocyte metabolites were secreted into the bile canaliculi, and then transported into the biliary structure. Hepatocytes in the organoid acquired and maintained metabolic functions including albumin secretion and cytochrome P450 activities, over the long term. In this study, we established functional liver tissue incorporating a bile drainage system *ex vivo*. This hepatobiliary organoid enabled us to reproduce the transport of hepatocyte metabolites in liver tissue, and to investigate the way in which the two types of epithelial cells establish functional connections.

Introduction

Epithelial organs consist of multiple types of epithelial tissue, such as alveoli and trachea in the lung, urinary tubules and collecting ducts in the kidney, acini and pancreatic ducts in the pancreas, and bile canaliculi (BC) and bile ducts (BDs) in the liver. The structures connecting two types of tissues are unique to each organ. Because various substances, including air, urine, digestive enzymes, and bile alter in composition as they flow through the connecting structures, it is crucial to accurately connect different tissue structures in order to reproduce the function of each organ *ex vivo*.

To generate organoids, or mini-organs, tissue stem cells are cultured in three-dimensions (3D), with the anticipation that they will self-organize into tissue structures similar to those found *in vivo*. This approach has been used to generate gastrointestinal functional units, including intestinal (1), gastric (2), colonic (3), and hepatic tissues (4, 5). The organoids are likely to contain niches for maintaining tissue stem/progenitor cells, given that these organoids can expand in size. However, the organoids consist of a single type of tissue, and do not contain structures connecting multiple types of epithelial cells.

Co-culturing is a technique used to generate organoids consisting of multiple types of tissues. A liver organoid equipped with a vascular system has been developed in a co-culture of hepatoblast-like cells, vascular endothelial cells, and mesenchymal cells, derived from human-induced pluripotent stem cells (hiPSCs) (6). The hepatocytes in the organoid may exchange metabolic substances via blood flow when they are transplanted into immunodeficient mice (7). However, the organoid does not contain the biliary structure that is essential to drain cytotoxic bile from the hepatic tissue.

In this study, we present a mouse hepatobiliary organoid with hepatocyte clusters derived from small hepatocytes (SHs) and a biliary network derived from epithelial cell adhesion molecule positive (EpCAM⁺) cholangiocytes. SHs are intrinsic hepatocyte progenitors isolated from healthy adult mice as hepatocytes with small size, which subsequently proliferate and differentiate into functional hepatocytes *in vitro* and *in vivo* (8, 9). In our hepatobiliary organoids, bilirubin and fluorescein-labeled bile acid were absorbed by the hepatocytes and accumulated in the biliary system, indicating that a connection between hepatocytes

and cholangiocytes had been established. Since hepatocyte clusters are functionally connected to the biliary tubules, we call this organoid a “hepatobiliary tubular organoid (HBTO)”. Hepatocytes in an HBTO acquired and maintained metabolic functions for more than one month. HBTOs enabled us to access the transport of hepatocyte metabolites within the liver tissue, and to monitor the metabolism of the hepatocytes in the long term *ex vivo*.

Results

Induction of hepatobiliary connections in co-cultures of hepatocytes and cholangiocytes.

In order to reconstruct hepatobiliary tissue structures *in vitro*, we used SHs and primary cholangiocytes isolated from healthy adult mice. SHs proliferate and differentiate into mature hepatocytes (MHs) in tissue culture dishes in the presence of Matrigel (MG) (**Fig. S1A**) (8, 9). SHs form BC-like structures, although they are not organized into a continuous luminal network (arrowheads in **Fig. S1A-1**). Primary cholangiocytes isolated as EpCAM⁺ cells proliferate on type I collagen gel, and form a tubular network with the overlay of collagen gel (**Fig. S1B**) (10, 11).

In order to generate multi-cellular tissue structures, spheroid or 3D cultures in which cell aggregates are embedded in MG are often used (12). Although hepatocytes generate bile canaliculi-like structures in spheroids (4), biliary networks are not generated in 3D culture, but are developed in sandwich culture (11, 13). Therefore, we used a sandwich culture in which type I collagen gel was used as the bottom layer, and type I collagen gel containing 20% MG (Col-MG) was used as the top layer, for co-culturing SHs and cholangiocytes. We mixed cholangiocytes and SHs and plated them onto type I collagen gel. Although the cholangiocytes and SHs formed colonies, they did not contact each other, and failed to form hepatobiliary connections. To establish contact between SHs and cholangiocytes, we added SHs to the culture after the cholangiocytes had proliferated to form colonies on the collagen gel (Fig. 1A). Under these conditions, SHs attached on empty spaces among cholangiocyte colonies, and close contact with cholangiocytes was established by one day after plating the SHs (Fig. [1B-1](#) and [2](#)). The HNF4 α ⁺ hepatocytes established tight junctions with the cholangiocytes (**Fig. S2-B** and **C**). Morphogenesis was induced by an overlay of Col-MG. Two weeks after the overlay, hepatocytes showed cellular morphology similar to that of mature hepatocytes, including a large amount of cytoplasm and round nuclei, and formed a BC network, whereas cholangiocytes formed a tubular network. At this stage, we identified luminal connections between hepatocytes and cholangiocytes under a phase-contrast microscope (Fig. [1B-3](#) and [4](#)). Immunofluorescence analysis performed four weeks after the Col-MG overlay further demonstrated that a luminal network formed within the HNF4 α ⁺ hepatocyte cluster (line a in Fig. [1C-1](#) and panels a-1 and a-2 of Fig. [1C](#)), that was connected to a lumen consisting of CK19⁺ cholangiocytes and HNF4 α ⁺ hepatocytes (line b in Fig. [1C-1](#) and panels b-1 and b-2), and then eventually to the duct of the CK19⁺ cholangiocytes (line c in Fig. [1C-1](#) and panels c-1 and c-2). In each experiment, we could observe hepatobiliary connections on the boundary between the cholangiocytes and the hepatocytes, using a phase-contrast

microscope. We evaluated the efficiency of the establishment of hepatobiliary connections in the organoids by staining with phalloidin and counting the lumen connecting the hepatocyte clusters and biliary tubules. We found 3.4 ± 0.4 connections (mean \pm SEM) per 1 mm of the boundary between hepatocytes and cholangiocytes. Since the hepatocyte clusters were connected to the biliary tubules, we called this organoid a “HBTO”.

Hepatocytes and cholangiocytes maintain their lineages to establish HBTOs

Recent research has shown that hepatocytes and cholangiocytes are plastic (15-18). The results shown in **Figure 1C** suggest that hepatocytes and cholangiocytes, but not any intermediate cells, form the hepatobiliary junctions. We further examined whether hepatocytes or cholangiocytes show intermediate characteristics, expressing both markers, to generate the hepatobiliary junctions. Antibodies against carcinoembryonic antigen related cell adhesion molecule (CEACAM) were used to specifically label the apical membrane of hepatocytes, and ezrin (EZN) was used to label cholangiocytes. As shown in **Figure 2A**, CEACAM⁺EZN⁻ hepatocytes (**closed arrowhead**) and CEACAM⁻EZN⁺ cholangiocytes (**open arrowhead**) formed the junction. We did not find CEACAM⁺EZN⁺ cells in the HBTOs. We also investigated the expression of CK19, Sry-HMG box 9 (SOX9), and osteopontin (OPN) as cholangiocyte markers, and radixin (RDX) as a hepatocyte marker (**Figs. 2A5 to 12 and S3**). The apical membranes of hepatocytes (**closed arrowheads**) and those of cholangiocytes (**open arrowheads**) surrounded the luminal space at hepatobiliary junctions. We did not find cells expressing both hepatocyte and cholangiocyte markers. As with the hepatobiliary connections observed in HBTO, CEACAM⁺EZN⁻ hepatocytes and CEACAM⁻EZN⁺ cholangiocytes surrounded the lumen at the hepatobiliary junction in adult liver tissue (**Fig. S4**).

There remains a possibility that hepatocytes were completely converted to cholangiocytes, or *vice versa*, during the generation of hepatobiliary connections. To examine whether lineage conversion is involved in hepatobiliary morphogenesis, we cultured SHs isolated from CAG-Cre:ROSA-tdTomato mice with wild type EpCAM⁺ cholangiocytes (**Fig. 2B**). The BC of Tomato⁺CK19⁻ hepatocytes (line a in panels 1-4 of **Fig. 2B** and panel 5-a) was connected to the lumen of Tomato⁻CK19⁺ biliary tissue (line c in panels 1-4 of **Fig. 2B** and panel 5-c). At the boundary, Tomato⁺CK19⁻ hepatocytes and Tomato⁻CK19⁺ cholangiocytes surrounded the luminal structure (line b in panels 1–4 of **Fig. 2B** and panel 5-b). Neither Tomato⁺ cholangiocytes nor Tomato⁻ hepatocytes were detected. We also cultured EpCAM⁺ cholangiocytes isolated from CAG-Cre:ROSA-tdTomato mice with SHs isolated from wild type mice (**Fig. S5**). In this culture, the BC network of hepatocytes (**closed arrowheads in Fig. S5A**) was connected to the biliary network of Tomato⁺ cholangiocytes (**open arrowheads in Fig. S5A**). Occasionally, some Tomato⁺ cholangiocytes were weakly positive for HNF4a, although their cellular morphology was visually identical to that of the neighboring cholangiocytes (**Fig. S5B**). Neither Tomato⁺ hepatocytes nor Tomato⁻ cholangiocytes were detected. Collectively, hepatocytes and cholangiocytes maintained their original lineages and formed the hepatobiliary connections, at least in HBTOs (**Table S1**).

Transport of hepatocyte metabolites in HBTOs

A variety of metabolic reactions occur within functional hepatocytes, and the metabolites produced are secreted into the BC and then transported into IHBDs. To demonstrate functional connections between hepatocytes and cholangiocytes, we investigated whether metabolites produced by hepatocytes were secreted into the BC and eventually transported into tubular structures consisting of cholangiocytes. We applied chloromethylfluorescein diacetate (CMFDA) to HBTOs and examined whether the compound accumulated in the biliary tissue. Hepatocytes, but not cholangiocytes, incorporated and degraded CMFDA to produce fluorescein, which was secreted into the apical luminal space (**Fig. S6A**). Fluorescein accumulates in the biliary tissue when hepatocytes and cholangiocytes establish functional connections. Fluorescein was detected at high levels in the BC network 10 min after incubation of HBTOs in medium containing CMFDA (**Figs. 3A-1 and 2**). Although some fluorescein was observed in the biliary network near the hepatocyte cluster at this time, more fluorescein was found to have been transported to the biliary tissue after 120 min of the incubation. We then added a fluorescein-labeled bile acid, cholyl-L-lysine fluorescein (CLF), to HBTOs, and followed its transport. CLF is incorporated into hepatocytes, but not cholangiocytes (**Fig. S6B**), and then secreted to the BC through the bile salt efflux pump. CLF was secreted to the BC by 30 min after the treatment, and had accumulated in the biliary tissue at 6 h (**Fig. 3B**), indicating that CLF secreted into the BC is transported to the biliary network. Finally, HBTOs were exposed to bilirubin and we investigated whether the bilirubin was metabolized and then accumulated in the biliary network. After five days of incubation, bilirubin in the luminal spaces of the HBTOs was visualized by oxidizing the bilirubin to biliverdin. Biliverdin was detected in both the biliary and the BC networks (**Fig. 3C**), indicating that the hepatocytes took up and modified bilirubin, which was then excreted to the BC and transported into the biliary network. These results indicate that the HBTOs reproduced the transport of hepatocyte metabolites in liver tissue *in vivo*.

Hepatocytes maintain metabolic functions in HBTOs

In order to provide an assay system for drug metabolism, it is important to induce the cellular characteristics of well-differentiated hepatocytes in the HBTOs. Hepatocytes in an HBTOs could secrete three times as much ALB as SH-derived hepatocytes (Hep) (**Fig. 4A**). HBTOs showed higher CYP1B1- and CYP3A4-like activity when compared with Hep (**Fig. 4B**). This CYP activity is comparable to that shown by MHs in culture (**Fig. S7**). HBTOs exhibited gradually increasing ALB secretion, and a high level of ALB secretion persisted for more than a month (**Fig. 4C**). Quantitative PCR data pertaining to *Cyp* expression (**Fig. S8**) and immunofluorescence in ALB (**Fig. S9**) indicated that CYP activity and ALB secretion were associated with hepatocytes, but not cholangiocytes, in HBTOs. Hepatocytes in HBTOs also absorbed DiI-AcLDL, a further indication that they were functional (**Fig. 4D**). The hepatobiliary connections in HBTOs promoted hepatic functions and contributed to maintaining these functions in the long term.

Cholangiocytes maintain secretory functions in the hepatobiliary organoid

Quantitative PCR analysis showed that cholangiocyte markers were expressed in HBTOs (**Fig. S10A**). Immunofluorescence analysis indicated that cholangiocyte markers, including EZN, CX19, SOX9, and OPN, were expressed in the cholangiocytes comprising HBTOs (**Figs. 2 and S3**). Rhodamine 123 was

incorporated into the biliary structure, depending on MDR activity (**Fig. S10B**). In response to forskolin, which increases the level of cAMP, the luminal spaces of the biliary network were expanded (**Fig. S10C**). These results indicate that cholangiocytes were functional in the HBTOs.

SHs are a subfraction of periportal and centrilobular hepatocytes

We established HBTOs using cholangiocytes and SHs. We tested MHs as a source of hepatocytes for HBTOs, but they did not form connections with cholangiocytes as efficiently as SHs (**Fig. 5A**). As we previously reported (8,9), SHs express typical hepatocyte markers, including *Hnf4a*, *Cps1*, and *Tdo2* (**Fig. S11A**). In order to further clarify the differences between SHs and MHs, gene expression profiles using RNA sequence were analyzed. The two types of hepatocyte showed very similar gene expression profiles, but the expression of *Cyp5* was lower in SHs than in MHs (**Fig. S11B**). Genes related to the Wnt signaling pathway were expressed at a lower level in SHs than in MHs (**Fig. S11C**). Hepatocytes can be categorized into three fractions—ZONE1, ZONE2, and ZONE3—depending on their localization on the tissue along the portal vein (PV) to the central vein (CV) axis (19). Using this categorization, the WNT/b-catenin signal was active in hepatocytes in ZONE3 (20, 21). Quantitative PCR analysis further demonstrated that WNT target genes such as *Gs*, *Lgr5* and *Axin2*, which are strongly expressed in ZONE3 hepatocytes, were only weakly expressed in SHs (**Fig. S11C**). *Cyp3a11* and *1a2* are also highly expressed in ZONE3 hepatocytes (21). These data strongly suggest that SHs are a subfraction of ZONE1 and ZONE2 hepatocytes. To investigate any correlation between the localization of SHs and their capability for establishing hepatobiliary connections with cholangiocytes, we tried to establish a protocol isolating hepatocytes in ZONE1 and ZONE2 from hepatocytes in ZONE3, and applied fractionated hepatocytes to an HBTO culture.

Membrane proteins are useful for distinguishing between different cellular populations. In the liver, E-cadherin (ECAD) is expressed in ZONE1 and ZONE2 hepatocytes, and claudin-2 (CLDN2) is expressed in ZONE3 hepatocytes (**Fig. 5B**). Consistent with the RNA sequence data, which indicated that SHs were in ZONE1 and ZONE2, SHs expressed more *Ecad/Cdh1* and less *Cldn2* than MHs (**Fig. 5C**). FACS analysis further demonstrated that SHs are strongly positive for ECAD, whereas MHs contain both ECAD⁺ and ECAD⁻ cells (**Figs. 5D**). ECAD⁺ MHs generated hepatobiliary connections with cholangiocytes more efficiently than did ECAD⁻ MHs (**Figs. 5E and F**). These results indicate that ECAD expression is required for hepatocytes to be involved in hepatobiliary connections with cholangiocytes, and that strong ECAD expression in SHs can explain their superiority over MHs for generating HBTOs.

Generation of hybrid HBTOs containing human hepatocytes

For pharmaceutical and clinical applications, human hepatocytes must be introduced into liver organoids. To this end, we applied human reprogramming hepatocytes (hCLiP), which can robustly differentiate to form functional hepatocytes *in vitro* (22), into co-culture with mouse cholangiocytes. When hCLiP were cultured alone, they differentiated into hepatocytes morphologically similar to MHs, but did not form BC-like structures (**Fig. 6A**). In co-culture with Tomato⁺ mouse cholangiocytes, BC-like

structures were evident (**Fig. 6B**). Immunofluorescence analysis demonstrated that the BC-like structure (line a in **Fig. 6B-1** and panels a-1&a-2) was connected to the biliary structure (line c in **Fig. 6B-1** and panels c-1 and c-2) via a lumen consisting of hepatocytes and cholangiocytes (line b in **Fig. 6B-1** and panels b-1 and b-2). When CLF was added to the medium, it accumulated in the luminal space, which consisted of Tomato⁺ cholangiocytes (**Fig. 6C**), indicating that human hepatocytes and mouse cholangiocytes can establish functional connections.

Discussion

To maintain healthy functional hepatocytes *in vitro* or *in vivo*, liver tissue must be equipped with a bile excretion system. In this report, we present HBTO, a hepatobiliary organoid, in which a BC network of hepatocytes connects to the biliary network. The hepatobiliary connection greatly contributes to the long term maintenance of functional hepatocytes.

To reproduce *in vivo* liver functions, in particular the transport of metabolites produced by hepatocytes, the liver tissue architecture should be implemented *ex vivo*. Liver organoids containing hepatocytes and cholangiocytes have been reported. However, the functions of these hepatocytes are not comparable to those of MHs, and the hepatobiliary connection remains unclear (23, 24). In this study, we have, for the first time, successfully constructed a hepatobiliary tissue structure *ex vivo* in which hepatocyte metabolites are transported from the BCs to BDs. In the process of determining the culture conditions, we first cultured SHs on 2, 4, and 6 mg/ml type I collagen gel, and found ALB secretion was at the highest level in culture using 4 mg/ml collagen gel. Therefore, we chose to use 4 mg/ml type I collagen as the bottom layer in HBTO culture. We counted hepatobiliary connections under a phase-contrast microscope, and found the largest number of connections when we used a collagen gel containing 20% MG as the top layer in HBTO culture as compared with collagen or MG alone.

The sequential plating of SHs and cholangiocytes, and the spontaneous induction of BD and BC morphogenesis, are key to establishing HBTOs. We mainly analyzed the structures and functions of HBTO three to four weeks after inducing morphogenesis, since at that time the hepatocytes had become functionally mature, as judged by ALB secretion. However, immunofluorescence analysis showed that the hepatocytes and cholangiocytes formed junctional structures by one week after Col-MG overlay (**Fig. S12A**). The nascent BC in the HNF4 α ⁺ hepatocyte cluster (**white arrowhead** in **Fig. S12A-5**) had already connected to the CK19⁺ biliary structure (**yellow arrowhead** in **Fig. S12A-5**). Comparing HBTO at one week and four weeks, it was evident that the BC network continued to extend beyond one week. This process is probably similar to hepatobiliary morphogenesis *in vivo*. At embryonic day 17 (E17), the hepatobiliary connections already exist (**yellow arrowheads** in **Fig. S12B-2**), although the BC network was still discontinuous (**white arrowheads** in **Fig. S12B-2**). In adult liver, the BC eventually form a continuous network, and the hepatobiliary system is established (**Fig. S12C**) (14). Therefore, HBTO could be useful for analyzing the process and regulatory mechanisms of hepatobiliary morphogenesis *in vitro*.

Recent reports have indicated that hepatocytes consist of several fractions of cells; SOX9⁺ hybrid hepatocytes (25) and Mfsd2a⁺ exist near the PV (26), whereas AXIN2⁺ hepatocytes are next to the CV (27). In addition to these subpopulations, our gene expression analysis suggested that SHs are a subfraction of hepatocytes in ZONE1 and ZONE2 (**Fig. S11**). Currently, the relationship between SHs and the previously reported hepatocyte subpopulations remains unclear, although SHs express *Sox9* at low levels (data not shown) and express less *Axin2* than MHs, consistent with the localization of SHs in ZONE1 and ZONE2, but not in ZONE3.

As is characteristic of hepatocytes in ZONE1 and ZONE2, SHs are ECAD⁺. This status may be crucial for generating hepatobiliary connections with ECAD⁺ cholangiocytes (**Fig. S13**), given that cadherin proteins form hemophilic interactions. SHs showed a higher proliferative capability than MHs, an ability which may be beneficial to the establishment of numerous contacts with cholangiocytes in co-culture before the induction of hepatobiliary morphogenesis. SHs expressed lower levels of *Cyp*s than MHs, and this characteristic was retained in HBTOs, as judged by the relatively low levels of *Cyp3a11* and *2e1* (**Fig. S8**). However, HBTOs derived from SHs show CYP3A4-like activity comparable to that of primary MHs, suggesting that SHs are mature in HBTOs (**Fig. S7**). Therefore, we consider that SHs are currently the preferred source of hepatocytes for generating HBTOs.

Liver transplantation is a curative therapy for fatal liver diseases. However, because of a shortage of donors, alternative therapies are always in demand, and hepatocyte transplantation has been considered as an alternative. Hepatocytes and hepatocyte-like cells derived from intrinsic and extrinsic stem/progenitor cells can repopulate the recipient liver in mouse and rat models (28, 29). In those experimental models, however, the proliferation of residual hepatocytes must be genetically or pharmacologically suppressed, a treatment which cannot be used in human patients, to allow transplanted cells to proliferate and become engrafted within the recipients' liver tissue. Liver organoids such as HBTOs may have advantages over hepatocytes; since HBTOs already contain clusters of functional hepatocytes, they do not have to expand in the recipient liver. HBTOs also contain a bile excretion system, which helps hepatocytes maintain their functions in the long term, without being affected by excess accumulation of cytotoxic bile. In future, it will be necessary to explore a method for introducing liver organoids into a recipient liver, and to develop techniques for connecting the biliary tissue in HBTOs to the BDs of recipients, to secure permanent bile drainage.

In this work, we established a new hepatobiliary organoid called an HBTO, in which the BC network in hepatocyte clusters is functionally connected to the biliary network. This new hepatobiliary organoid paves the way for the generation of a system for directly monitoring the flux of hepatocyte metabolites within the liver tissue *ex vivo*. By exploring ways to collect hepatocyte metabolites from biliary tissue, an assay system for drug metabolism could be established. HBTOs containing human hepatocytes such as hCLiPs are useful for research into liver injuries and the development of new drugs. Our results provide a basic concept, and a system, for generating functional liver tissue *ex vivo*.

Materials And Methods

Mice

C57BL6 mice were purchased from Sankyo Labo Service Corporation, Inc. (Tokyo, Japan). CAG-Cre:ROSA-LSL-tdTomato mice were obtained by crossing B6.Cg-Tg(CAG-Cre)CZ-MO20sb (CAG-Cre) mice from Riken BRC (30) with B6.Cg-Gt(ROSA)26Sortm(CAG-tdTomato)Hze/J (ROSA-LSL-tdTomato) mice (The Jackson Laboratory, Bar Harbor, ME). Eight to twelve weeks old mice were used for cell isolation. All animal experiments were approved by the Sapporo Medical University Institutional Animal Care and Use Committee and were conducted according to institutional guidelines for ethical animal use.

Culture materials

High concentration type I collagen, and growth factor reduced Matrigel (MG) were purchased from Corning (Corning, NY). Epidermal growth factor (EGF) and hepatocyte growth factor (HGF) were purchased from Corning. Oncostatin M (OSM) was purchased from R&D systems (Minneapolis, MN). Tissue culture plates (24 well) were purchased from Greiner Bio-One (Kremsmünster, Austria). DMEM/F-12 medium (Sigma-Aldrich, St. Louis, MO) supplemented with 10% FBS (MP Biomedicals, Santa Ana, CA), 10 mM nicotinamide (Sigma-Aldrich), 1×10^{-7} M dexamethasone (Dex, Sigma-Aldrich), and 1× ITS (Gibco, Grand Island, NY) was used as the basic medium. The growth medium was prepared by adding 5 ng/ml EGF and 5 ng/ml HGF to the basic medium. The differentiation medium was prepared by adding 1% DMSO (Sigma-Aldrich) to the basic medium.

Cell Isolation

To isolate hepatocytes and cholangiocytes from adult mouse liver, two-step collagenase perfusion was performed, as previously reported (9, 10). MHs and SHs were obtained from digested tissue, whereas undigested tissue was kept for isolating cholangiocytes. After collagenase perfusion, the cell suspension was centrifuged at $50 \times g$ for 1 min. The pellet was suspended in Hanks' balanced salt solution, mixed with Percoll and centrifuged at $50 \times g$ for 15 min to eliminate dead cells, yielding MHs. The supernatant collected after centrifugation at $50 \times g$ was further centrifuged at $115 \times g$ for 3 min. The pellet was suspended in Hanks' balanced salt solution, mixed with Percoll and centrifuged at $180 \times g$ for 15 min to eliminate dead cells, yielding SHs. The residual tissue after collagenase perfusion was further digested with collagenase/hyaluronidase solution. Liberated cells were used for isolating cholangiocytes, based on the expression of EpCAM, by a magnetic cell sorter (MACS) (Miltenyi Biotec, Bergisch Gladbach, Germany).

Induction of the HBTOs

Cholangiocytes were resuspended in the growth medium and plated in 24-well plates coated with 200 ml of 4 mg/ml type I collagen gel prepared from high concentration type I collagen (Corning) at a density of 50,000 cells/well. Five days after plating, SHs were added to each well at a density of 50,000 cells/well. Following a further two days of incubation, the medium was replaced with differentiation medium

supplemented with 10 ng/ml oncostatin M (OSM), and then overlaid with collagen gel containing 20% MG (Col-MG), which was prepared by mixing 2 mg/ml type I collagen gel and MG (v/v=4:1) on ice. The plate was incubated at 37°C for 3–4 h to form a gel, and then the differentiation medium was added. Culture medium was replaced with fresh medium every four days.

Immunostaining and confocal imaging

A sandwich culture was fixed in PBS containing 4% paraformaldehyde at 4°C for 30 min with gentle shaking. After washing with PBS, the samples were permeabilized in PBS containing 1% Triton X-100 at room temperature for 30 min. After blocking in Block ACE containing 0.1% Triton X-100, the samples were incubated with primary antibodies and then dye-conjugated secondary antibodies were applied. Nuclei were counterstained with Hoechst33342. The primary and secondary antibodies used for immunostaining are listed in **Tables S2** and **S3**. Images were acquired using Zeiss LSM780 confocal laser scanning microscopes (Carl Zeiss, Jena, Germany) and Olympus FV3000 microscopes (Olympus, Tokyo, Japan).

Identification and quantification of the hepatobiliary connections in HBTOs

HBTOs were stained with phalloidin, anti-CK19, and anti-HNF4a antibodies, and then the phalloidin (+) luminal structures connecting CK19(+) ducts with HNF4a(+) hepatocyte clusters were counted. The same images were used to measure the boundary between hepatocyte clusters and the biliary tissue using Olympus cellSens software. Three to four different areas in four independent experiments were examined using the same method.

Uptake of chloromethyl fluorescein diacetate (CMFDA) and cholyl-lysine fluorescein (CLF)

Three to four weeks after Col-MG overlay, the medium was replaced with a differentiation medium containing 1 mg/ml CMFDA (FUJIFILM Wako Pure Chemical Corporation, Osaka, Japan) or 1 mg/ml CLF (Corning). The wells were washed with the differentiation medium five times, after 10 min incubation with CMFDA and 30 min incubation with CLF. Images were taken with an Olympus fluorescence microscope. Three to four areas per well were selected, and the transport of CMFDA and CLF was examined by taking fluorescence and phase-contrast images at different time points. Experiments were repeated three times. Representative images are shown in **Figure 3**.

Detection of bilirubin in the organoids

Ten mg of bilirubin (Kanto Chemicals, Tokyo, Japan) was dissolved in 0.1 ml of DMSO. Then 200 ml of 0.1 M Na₂CO₃, 500 ml of FBS, 20 ml of 0.1 N HCl, and 180 ml of distilled water were added. The solution was diluted ten-fold with DMSO. The bilirubin solution was further diluted 100-fold with culture medium, to produce a 10 mg/ml bilirubin solution, which was then filtered using a pore size of 0.22 μm (31). HBTOs were incubated with a medium containing 10 mg/ml bilirubin for five days. Hall's method (32) was used for the histochemical staining of bilirubin. The organoids were washed with PBS and fixed with

10% buffered neutral formalin for 5 min at room temperature, and then washed twice with distilled water. Fouchet's reagent, containing 22.5% trichloroacetic acid and 1% ferric chloride, was added and the mixture was incubated at room temperature for 5–15 min, until green biliverdin was detected in the luminal networks of the organoids. Bilirubin detection was repeated three times at three or four weeks after Col-MG overlay. A representative image is shown in **Figure 3**.

ALB ELISA

Sandwich ELISA using goat anti-mouse ALB (Bethyl Laboratories, Montgomery, TX) and HRP-conjugated anti-mouse ALB antibodies (Bethyl Laboratories) was performed to measure ALB in the culture medium. Signal was detected with o-Phenylenediamine (OPD) (Sigma-Aldrich) and measured on an 800TS absorbance reader (BioTek, Winooski, VT). The HBTOs were kept for two to three months, and the ALB concentration in the culture medium was measured using ELISA every two weeks after Col-MG overlay. The long term culture for 8 weeks after Col-MG overlay was repeated three times. One out of three cultures were extended for additional 4 weeks. As a control, SHs were plated onto collagen gel in 24-well plates at a density of 5×10^4 cells/well and overlaid with Col-MG.

CYP activity

CYP activity was measured using Glo-CYP3A4-Assay and Glo-CYP1B1-Assay (Promega, Madison, WI). The substrate was added to the culture medium at the concentration shown in the protocol, and incubated for 30 min for CYP3A4 and 3 hours for CYP1B1. Assays using four wells per experiment were repeated twice for CYP1B1 and three times for CYP3A4. The average values of representative cultures are shown in **Figure 4**. As a control, SHs were cultured in a sandwich culture as HBTOs, and the CYP activity was examined.

Uptake of low density lipoprotein (LDL)

Four weeks after Col-MG overlay, HBTOs were incubated with the growth medium containing 2 mg/ml Dil-acetylated LDL (Alpha Acer, Havehill, MA) for 1 hour. Wells were washed with the growth medium twice, and images were taken with an Olympus fluorescence microscope. Uptake of LDL was examined twice and the representative images are shown in **Figure 4**.

Quantitative PCR

MHs and SHs were isolated as described above in "Cell Isolation". SHs were further purified by isolating CD31⁻CD45⁻EpCAM⁺ICAM-1⁺ cells using a FACSAriaII (9). Total RNA was extracted and used for synthesizing cDNA using PrimeScript 1st strand cDNA synthesis kits (Takara Bio Inc., Shiga, Japan). Quantitative PCR was performed using an ABI PRISM 7500 (Thermo Fisher, Scientific) with the primers 5'-atcctcgccctgctgatt-3' and 5'-accaccgttctcctccgta-3' for *Cdh1*, and 5'-tgtgaatgaactgaaggaaagc-3' and 5'-atcctgcaccagctgtatt-3' for *Cldn2*. Isolation of MHs and SHs was repeated four times and purified MHs and SHs were used for 1st strand cDNA synthesis and for quantitative PCR.

Separation of ECAD(+) MHs

MHs were incubated with PE-conjugated anti-ECAD antibody (BioLegend). ECAD(-) and (+) MHs were isolated using a FACSaria II. Five days before cell isolation, cholangiocytes were plated on type I collagen gel. Isolated MHs were plated onto collagen gel containing cholangiocyte colonies. Cell isolation and co-culture was repeated three times. The number of hepatobiliary connections was examined after staining with antibodies against HNF4a & CK19, phalloidin, and Hoechst 33342.

Culture of human reprogramming hepatocytes (hiCLiP)

hCLiPs were generated from primary human hepatocytes, as previously reported (22). For inducing hybrid HBTO, mouse cholangiocytes isolated from Tomato mice were plated on type I collagen gel. On the same day, a frozen stock of hCLiP was thawed and the hCLiPs were kept on dishes coated with type I collagen. On day 5, hCLiPs were treated with trypsin-EDTA and, after centrifugation, the cells were plated onto collagen gel, where cholangiocytes formed colonies. Two days after the hCLiPs were plated, 10 ng/ml human OSM was added to the culture, followed by an overlay of collagen gel containing 40% MG. The co-culture was repeated four times. Representative data are shown in **Figure 6**.

Statistical analysis

Unpaired two-tailed student t-tests were performed for the data pertaining to CYP1B1&CYP3A4 activity, ALB secretion, quantification of the number of hepatobiliary connections, and qPCR data using Microsoft Excel.

Declarations

Acknowledgments

We thank Ms. Yumiko Tsukamoto for technical assistance. We also thank Enago (www.enago.jp) for the English language review.

Funding

This work was supported by the Ministry of Education, Culture, Sports, Science and Technology, Japan, Grants-in-Aid for Scientific Research (C) for N. Tanimizu (25460271, 16K08716), Grants-in-Aid for Scientific Research on Innovative Areas “Stem Cell Aging and Disease” for N. Tanimizu (17H05653), Grants-in-Aid for Scientific Research (B) for T. Mitaka (18H02873), and Grants-in-Aid for Exploratory Research for T. Mitaka (26670584, 17K19703). This work was also supported by Research Grant from Hokkaido hepatitis foundation.

Author Contributions

N.T.: Writing (Original draft), **Conceptualization, Investigation, Methodology**

N.I.: Data Discussion, Writing (Review)

Y.S.: Data Curation, Formal analysis

T.I.: Writing (Review and Editing), Resources

R.S.: Writing (Editing), Resources

T.Y.: Resources

T.K.: Resources

T.T.: Data Curation, Formal analysis

T.O.: Resources

A.M.: Data Discussion, Resources

T.M.: Writing (Review and Editing), Funding acquisition

References

1. Sato, T. *et al.*, Single Lgr5 stem cells build crypt-villus structures in vitro without a mesenchymal niche. *Nature* **459**, 262 (2009).
2. Noguchi, T. K. *et al.*, Generation of stomach tissue from mouse embryonic stem cells. *Nat. Cell Biol.* **17**, 984 (2015).
3. Yui, S. *et al.*, Functional engraftment of colon epithelium expanded in vitro from a single adult Lgr5(+) stem cell. *Nat. Med.* **18**, 618 (2012).
4. Hu, H. *et al.*, Long-Term Expansion of Functional Mouse and Human Hepatocytes as 3D Organoids. *Cell* **175**, 1591 (2018).
5. Peng, W. C. *et al.*, Inflammatory Cytokine TNF alpha Promotes the Long-Term Expansion of Primary Hepatocytes in 3D Culture. *Cell* **175**, 1607 (2018).
6. Takebe, T. *et al.*, Massive and Reproducible Production of Liver Buds Entirely from Human Pluripotent Stem Cells. *Cell Rep.* **21**, 2661 (2017).
7. Takebe, T. *et al.*, Vascularized and functional human liver from an iPSC-derived organ bud transplant. *Nature* **499**, 481 (2013).
8. Mitaka, T. *et al.* Reconstruction of hepatic organoid by rat small hepatocytes and hepatic nonparenchymal cells. *Hepatology* **29**, 111 (1999).
9. Tanimizu, N. *et al.*, Liver progenitors isolated from adult healthy mouse liver efficiently differentiate to functional hepatocytes in vitro and repopulate liver tissue. *Stem Cells* **34**, 2889 (2016).
10. Tanimizu, N. *et al.*, Hepatic biliary epithelial cells acquire epithelial integrity but lose plasticity to differentiate into hepatocytes in vitro during development. *J. Cell Sci.* **126**, 5239 (2013).

11. Hashimoto, W. *et al.*, Ductular network formation by rat biliary epithelial cells in the dynamical culture with collagen gel and dimethylsulfoxide stimulation. *Am. J. Pathol.* **173**, 494 (2008)
12. Clevers, H. Modeling development and disease with organoids. *Cell* **165**, 1586 (2016)
13. Tanimizu, N. *et al.*, Liver progenitor cells develop cholangiocyte-type epithelial polarity in three-dimensional culture. *Mol Biol. Cell* **18**, 1472 (2007)
14. Tanimizu, N. *et al.*, Intrahepatic bile ducts are developed through formation of homogeneous continuous luminal network and its dynamic rearrangement in mice. *Hepatology* **64**, 175 (2016).
15. Yanger, K. *et al.*, Robust cellular reprogramming occurs spontaneously during liver regeneration. *Genes Dev.* **27**, 719 (2013).
16. Tanimizu, N. *et al.* Sry HMG box protein 9-positive (Sox9⁺) epithelial cell adhesion molecule-negative (EpCAM⁻) biphenotypic cells derived from hepatocytes are involved in mouse liver regeneration. *J Biol. Chem.* **289**, 7589 (2014).
17. Tarlow, B. D. *et al.*, Bipotential adult liver progenitors are derived from chronically injured mature hepatocytes. *Cell stem cell* **15**, 605 (2014).
18. Raven, A. *et al.*, Cholangiocytes act as facultative liver stem cells during impaired hepatocyte regeneration. *Nature* **547**, 350 (2017).
19. Ben-Moshe, S. and Itzkovitz, S. Spatial heterogeneity in the mammalian liver. *Nat. Rev. Gastroenterol. Hepatol.* **16**, 395 (2019).
20. Benhamouche, S. *et al.*, Wnt/beta-catenin pathway and liver metabolic zonation: a new player for an old concept. *Medicine Sci.* **22**, 904 (2006).
21. Sekine, S. *et al.*, Liver-specific loss of beta-catenin blocks glutamine synthesis pathway activity and cytochrome p450 expression in mice. *Hepatology* **43**, 817 (2006).
22. Katsuda, T. *et al.*, Generation of human hepatic progenitor cells with regenerative and metabolic capacities from primary hepatocytes. *Elife* **8**, e47313 (2019)
23. Wu, F. *et al.*, Generation of hepatobiliary organoids from human induced pluripotent stem cells. *J. Hepatol.* **70**, 1145 (2019).
24. Vyas, D. *et al.*, Self-assembled liver organoids recapitulate hepatobiliary organogenesis in vitro. *Hepatology* **67**, 750 (2018).
25. Font-Burgada, J. *et al.*, Hybrid Periportal Hepatocytes Regenerate the Injured Liver without Giving Rise to Cancer. *Cell* **162**, 766 (2015).
26. Wang, B. *et al.* Self-renewing diploid Axin2(+) cells fuel homeostatic renewal of the liver. *Nature* **524**, 180 (2015)
27. Pu, W. *et al.*, Mfsd2a⁺ hepatocytes repopulate the liver during injury and regeneration. *Nat. Commun.* **7**, 13369 (2016)
28. Katsuda, T. *et al.*, Conversion of Terminally Committed Hepatocytes to Culturable Bipotent Progenitor Cells with Regenerative Capacity. *Cell Stem Cell* **20**, 41–55 (2017)
29. Grompe, M. *Adv. Exp. Med. Biol.* **959**, 215–30 (2017)

30. Matsumura, H. *et al.*, Lineage-specific cell disruption in living mice by Cre-mediated expression of diphtheria toxin A chain *Biochem. Biophys. Res. Commun.* **321**, 275–9 (2004)
31. Sudo, R. *et al.*, Bile canalicular formation in hepatic organoid reconstructed by rat small hepatocytes and nonparenchymal cells. *J Cell Physiol.* **199**, 252–61 (2004)
32. HALL, M.H. *et al.*, A staining reaction for bilirubin in sections of tissue *Am. J. Clin. Pathol.* **34**, 313–6 (1969)

Figures

Fig. 1

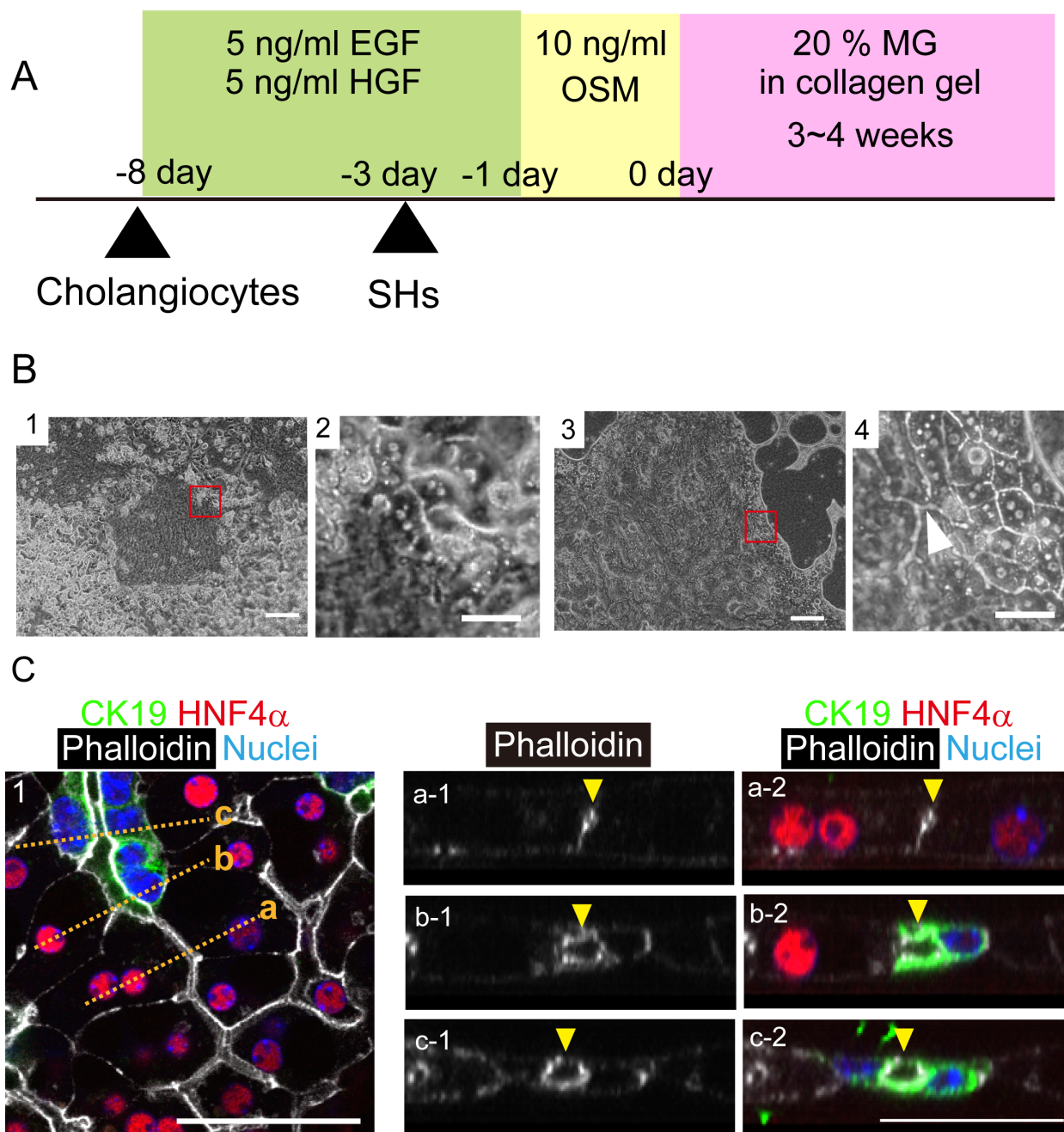


Figure 1

Induction of hepatobiliary connections in co-cultures of SHs and cholangiocytes. A. Schedule of co-culture of cholangiocytes and small hepatocytes. B. Morphological changes of hepatocytes and cholangiocytes in co-culture. Cholangiocytes are in close contact with hepatocytes one day after plating SHs (panels 1 and 2). At two weeks after overlay of collagen-containing 20% Matrigel (MG), the BC network of hepatocytes connects to that of the biliary network (arrowhead in panel 4). Boxes in panels 1 and 3 are enlarged in panels 2 and 4, respectively. Bars in panels 1&3 and 2&4 represent 200 and 50 μm , respectively. C. Hepatobiliary connections in co-culture. The bile canaliculi within the HNF4 α + hepatocyte clusters (line a in Fig. 1C-1, and Figs. 1C-2a and 1C-3a) connect to the lumen, which consists of CK19+ cholangiocytes and HNF4 α + hepatocytes (line b in Fig. 1C-1, and Figs. 1C-2b and 1C-3b), and then eventually reach the duct of CK19+ cholangiocytes (line c in Fig. 1C-1, and Figs. 1C-2c and 1C-3c). Lumens are indicated by arrowheads. Boxes in panels 1 and 6 are enlarged in panels 2–5 and panels 7–10, respectively. At four weeks after MG overlay, the hepatobiliary organoid was fixed and stained with phalloidin, anti-HNF4 α , and anti-CK19 antibodies. Bars represent 50 μm .

Fig. 2

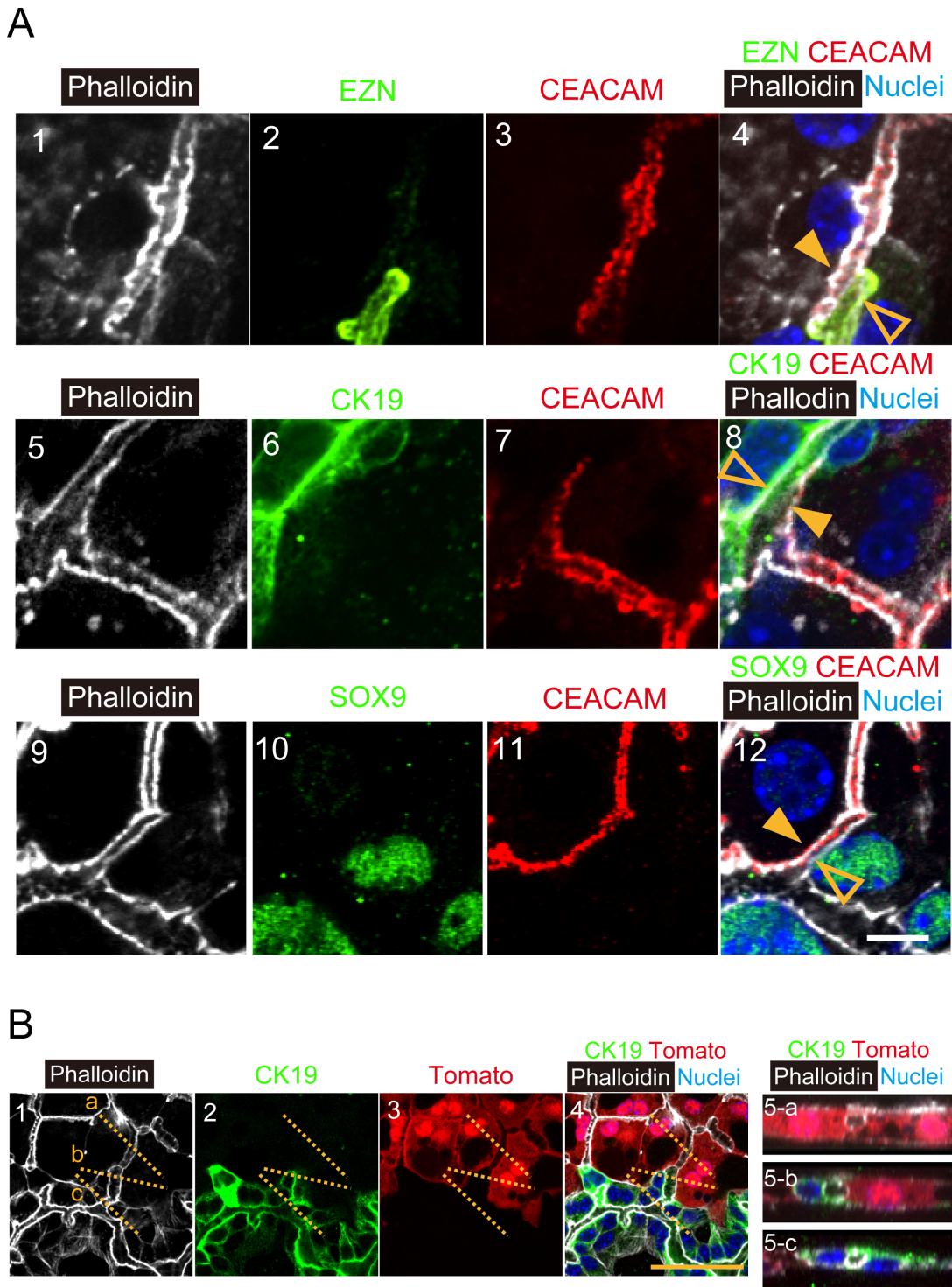


Figure 2

Hepatocytes and cholangiocytes maintain their lineage to establish hepatobiliary junctions. A. Immunological identification of the hepatobiliary junction. The hepatobiliary junction consists of hepatocytes (closed arrowheads) and cholangiocytes (open arrowheads). The continuous lumen stained with phalloidin is surrounded by CEACAM+EZN⁻ hepatocytes and CEACAM⁻EZN⁺ cholangiocytes (panels 1–4), CEACAM+CK19⁻ hepatocytes and CEACAM⁻CK19⁺ cholangiocytes (panels 5–8), or

CEACAM+SOX9⁻ hepatocytes and CEACAM⁻SOX9⁺ cholangiocytes (panels 9–12). B. Tomato⁺ hepatocytes maintain their lineage to form a continuous luminal network with cholangiocytes. The luminal network among Tomato⁺ hepatocytes (line a in panels 14 and panel 5a) is connected to that of the Tomato⁻CK19⁺ biliary structure (line c in panels 14 and panel 5c) at the boundary (line b in panels 14 and panel 5b). The luminal network is recognized by F-actin bundles visualized using phalloidin. Bars represent 50 μ m.

Fig. 3

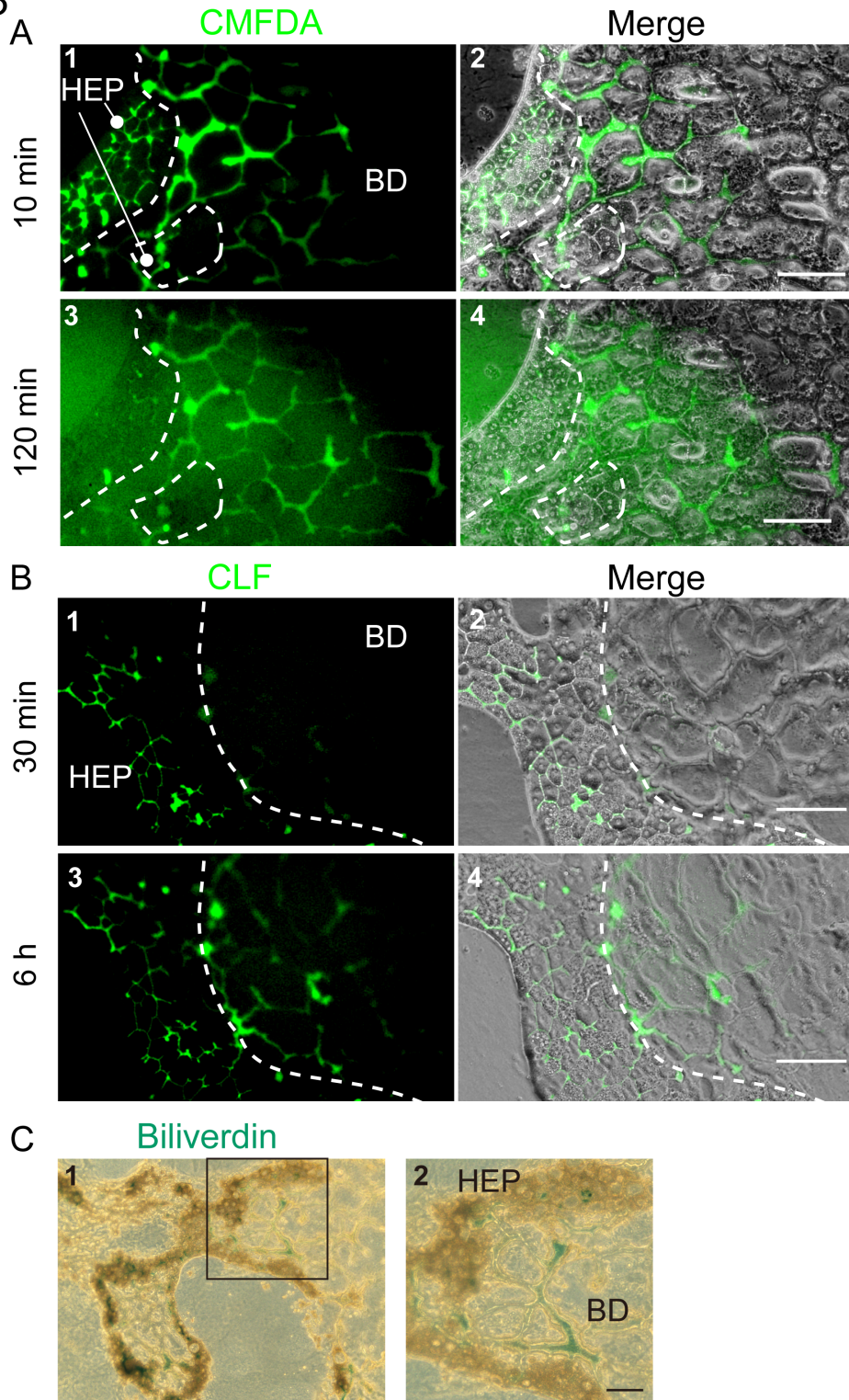


Figure 3

Transport of hepatocyte metabolites in HBTO. A. Transport of fluorescein diacetate in HBTOs. Fluorescein derived from chloromethyl fluorescein diacetate (CMFDA) is secreted into BCs and then transported into the biliary network. After 10 min of incubation, fluorescein is strongly detected in the BC network of the hepatocyte cluster (HEP, surrounded by dotted line) as well as in the biliary network (BD). Fluorescein is absent from the hepatocyte clusters and reaches the biliary network after 120 min incubation. HBTOs were incubated in the presence of CMTFDA for 10 min. Phase-contrast and fluorescent images were taken after washing with culture medium five times. HBTOs were kept in the culture medium without CMTFDA. Dotted lines indicate the boundary between HEP and BD. Scale bars represent 100 μm . B. Transport of bile acids in HBTO. CLF taken up by hepatocytes is transported into the biliary network. The organoids were incubated in the presence of CLF for 30 min. After five washes, images were taken at 30 min (panels 1&2) and at 6 hours (panels 3&4). Dotted lines indicate the boundary between HEP and BD. Scale bars represent 100 μm . C. Transport of bilirubin. Bilirubin taken up by hepatocytes is excreted into BCs and then transported into the biliary network. Bilirubin in HBTOs was visualized by turning it into biliverdin. A scale bars represent 100

Transport of hepatocyte metabolites in HBTO. A. Transport of fluorescein diacetate in HBTOs. Fluorescein derived from chloromethyl fluorescein diacetate (CMFDA) is secreted into BCs and then transported into the biliary network. After 10 min of incubation, fluorescein is strongly detected in the BC network of the hepatocyte cluster (HEP, surrounded by dotted line) as well as in the biliary network (BD). Fluorescein is absent from the hepatocyte clusters and reaches the biliary network after 120 min incubation. HBTOs were incubated in the presence of CMFDA for 10 min. Phase-contrast and fluorescent images were taken after washing with culture medium five times. HBTOs were kept in the culture medium without CMFDA. Dotted lines indicate the boundary between HEP and BD. Scale bars represent 100 μm . B. Transport of bile acids in HBTO. CLF taken up by hepatocytes is transported into the biliary network. The organoids were incubated in the presence of CLF for 30 min. After five washes, images were taken at 30 min (panels 1&2) and at 6 hours (panels 3&4). Dotted lines indicate the boundary between HEP and BD. Scale bars represent 100 μm . C. Transport of bilirubin. Bilirubin taken up by hepatocytes is excreted into BCs and then transported into the biliary network. Bilirubin in HBTOs was visualized by turning it into biliverdin. A scale bars represent 100 μm .

Fig. 4

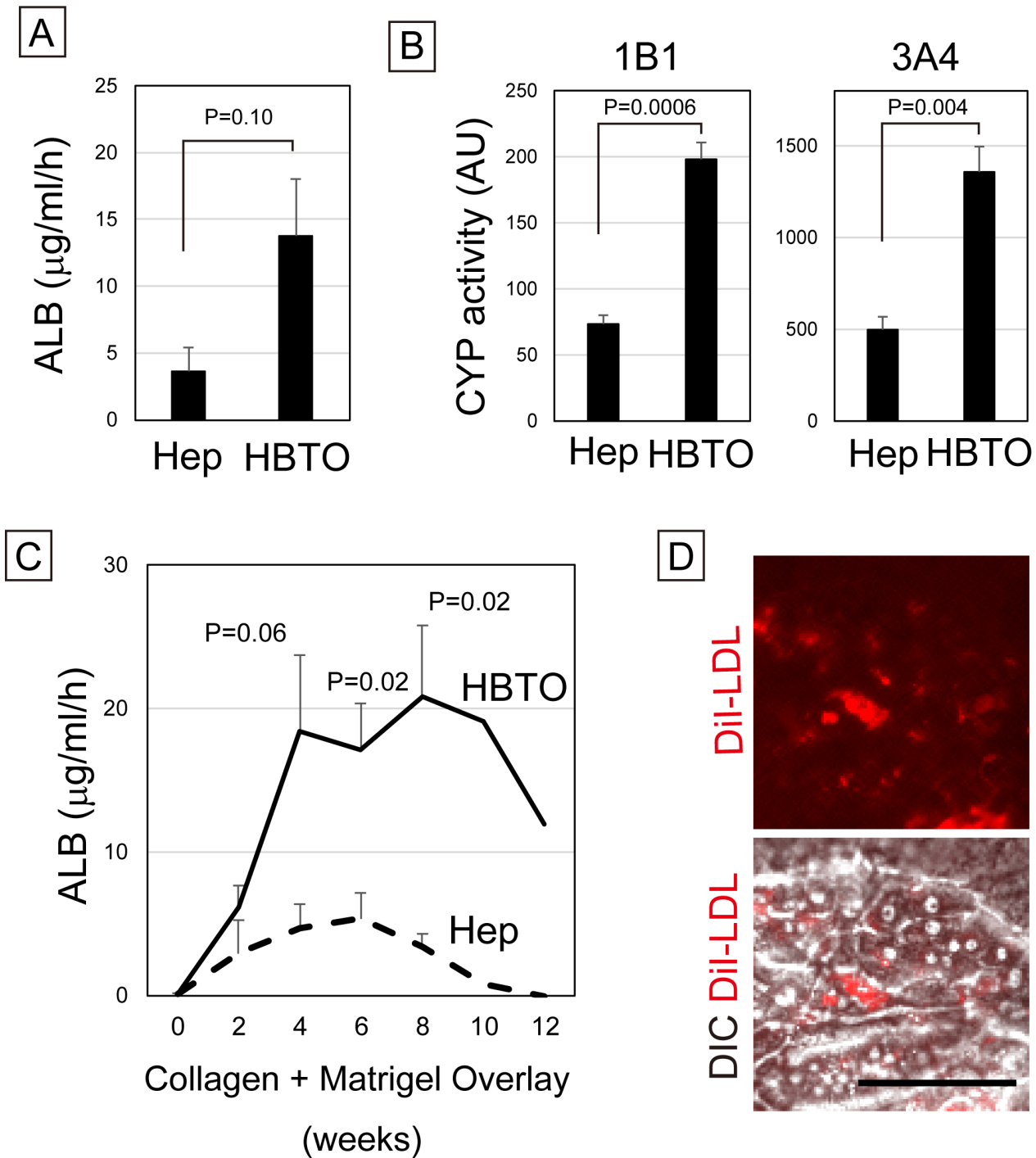


Figure 4

Hepatocytes maintain metabolic functions in HBTO. A. ALB secretion from hepatocytes and HBTOs. Hepatocytes in HBTOs secrete more ALB than those cultured alone. SHs were plated onto collagen gel with or without cholangiocyte colonies. Culture medium was collected, and ALB concentration was examined by ELISA four weeks after gel overlay. Error bars represent SEM. B. Activity of cytochrome P450s in hepatocytes and HBTOs. Hepatocytes in HBTOs show higher levels of CYP1B1, and 3A4 activity

than those cultured alone. CYP activities were examined three weeks after the overlay of collagen gel. The average values of CYP activity measured for three independent cultures are shown in the graphs. Error bars represent SEM. C. Long term maintenance of ALB secretion. ALB secretion gradually increases for four weeks after gel overlay. Then, hepatocytes in HBTO maintain ALB secretion at a similar level for the following three to four weeks. ALB secretion was observed for two months for three independent cultures; average values with SEM at each time point during two- month period are shown in this figure. One culture was further extend to measure ALB secretion at ten and twelve weeks after Col-MG overlay. D. Hepatocytes in HBTOs take up low density lipoprotein (LDL). Hepatocytes in HBTOs can take up Dil-AcLDL in supplemented culture medium. HBTOs were maintained for four weeks and further incubated in the presence of Dil-AcLDL for 1 hour. Bars represent 100 μ m.

Fig. 5

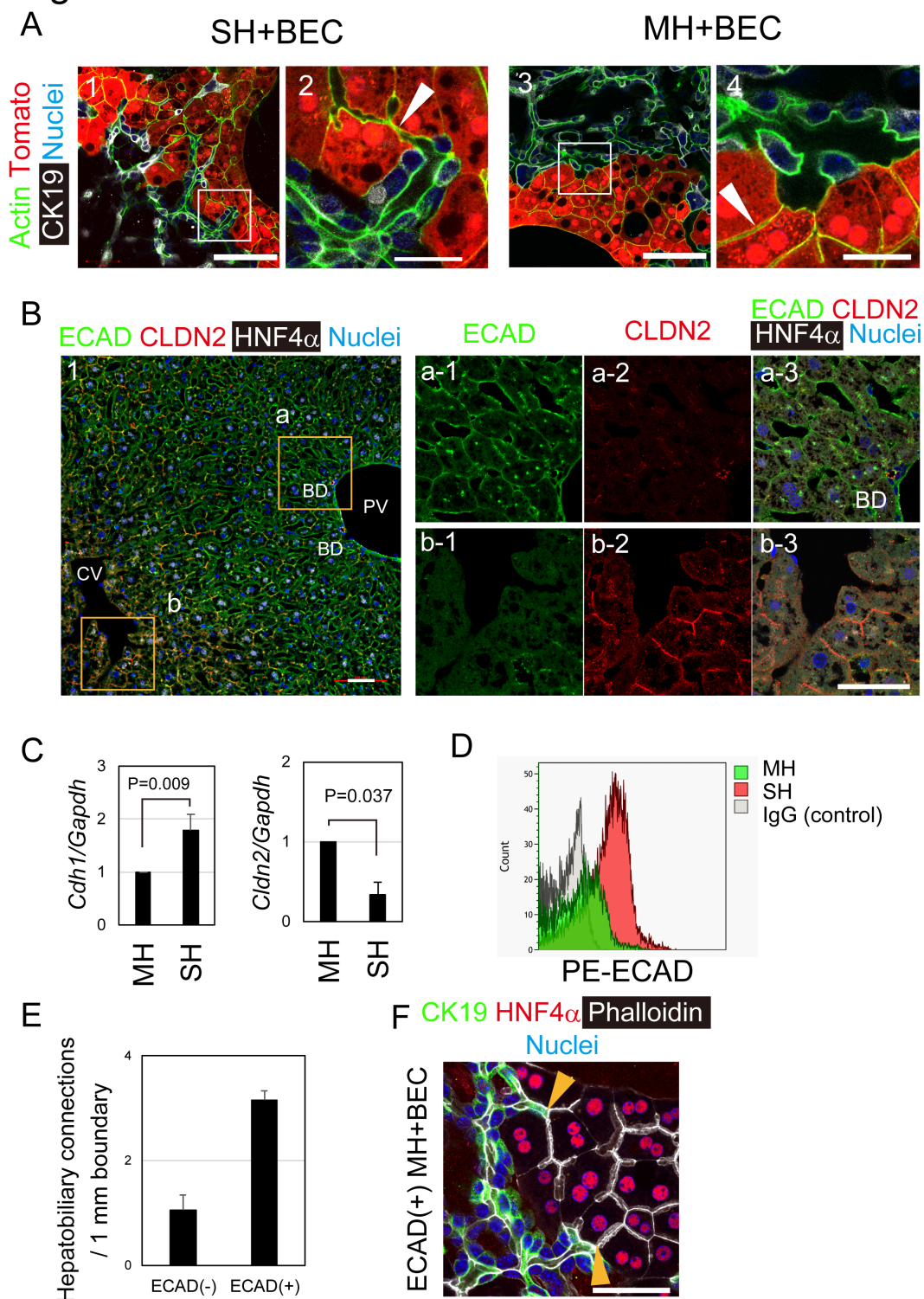


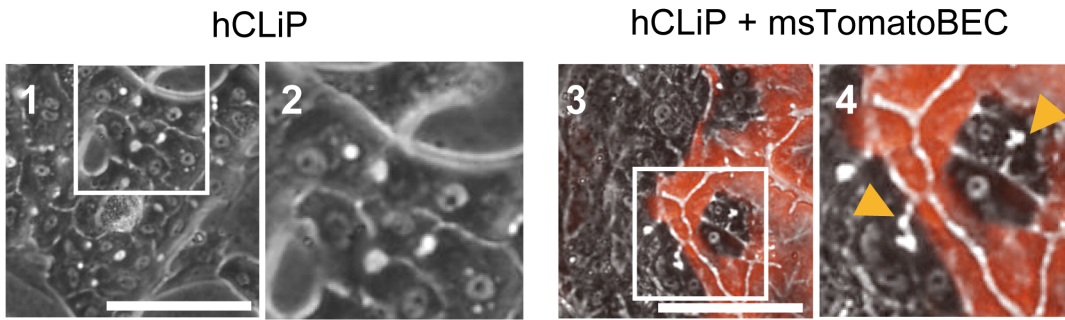
Figure 5

ECAD+ hepatocytes form hepatobiliary junctions with cholangiocytes. A. SHs, but not MHs, efficiently form hepatobiliary connections with cholangiocytes at their boundaries. The BCs of Tomato+ SHs (white arrowhead in panel 2) connect to CK19+ BD. MHs contact cholangiocytes, but their BC (white arrowhead in panel 4) does not connect to BD. Boxes in panels 1 and 3 are enlarged in panels 2 and 4, respectively. Bars in panels 1 and 3 represent 100 μ m and those in panels 2 and 4 represent 20 μ m. B. ECAD is

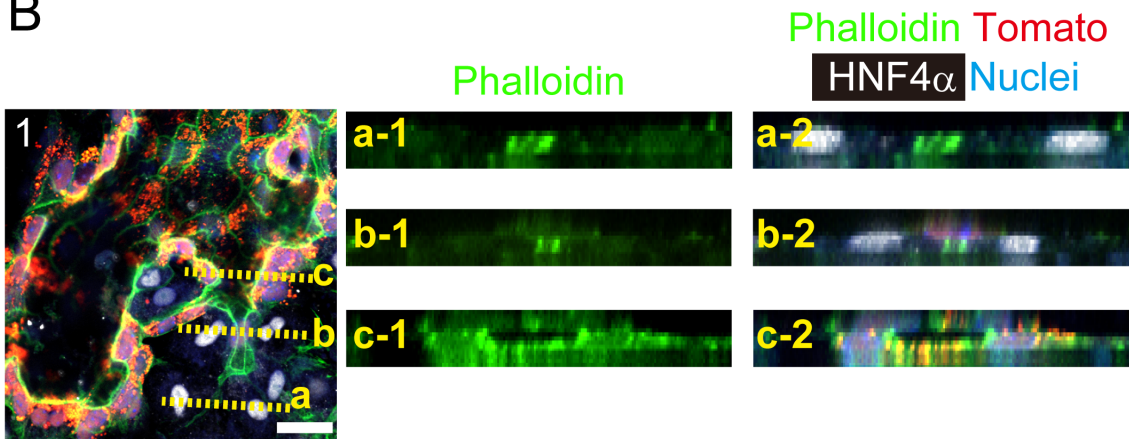
expressed in ZONE1&2 and CLDN2 in ZONE3 hepatocytes in the adult liver. Hepatocytes in ZONE1&2 are ECAD+CLDN2- (panels a1~a3), whereas those in ZONE3 are ECAD-CLDN2+ (panels b1~b3). An adult liver section was stained with anti-ECAD (green), anti-CLDN2 (red), and anti-HNF4 α (white) antibodies. Nuclei were counterstained with Hoechst 33342. Boxes in panel 1 are magnified in panels a1 to a3 and b1 to b3. Scale bars represent 50 μ m. C. SHs express more Cdh1 and less Cldn2 than MHs. qPCR analysis shows that Cldn2 is expressed at a lower level in SHs than in MHs. Cdh1/Ecad is higher in SHs than in MHs. MHs and SHs were isolated from six mice independently, and used for cDNA synthesis. Bars represent SEM. D. ECAD expression patterns are different in SHs and MHs. FACS analysis shows that all SHs are ECAD+, whereas MHs consist of both ECAD- and ECAD+ cells. MHs and SHs were incubated with PE-conjugated anti-ECAD antibody, and ECAD expression was examined using a FACS Aria equipped with a green laser. E. ECAD+ MHs form hepatobiliary junctions. ECAD+ MHs form hepatobiliary junctions with cholangiocytes more efficiently than ECAD- MHs. Unpaired two-tailed t-tests were performed using Microsoft Excel. Bars represent SEM.

Fig. 6

A



B



C

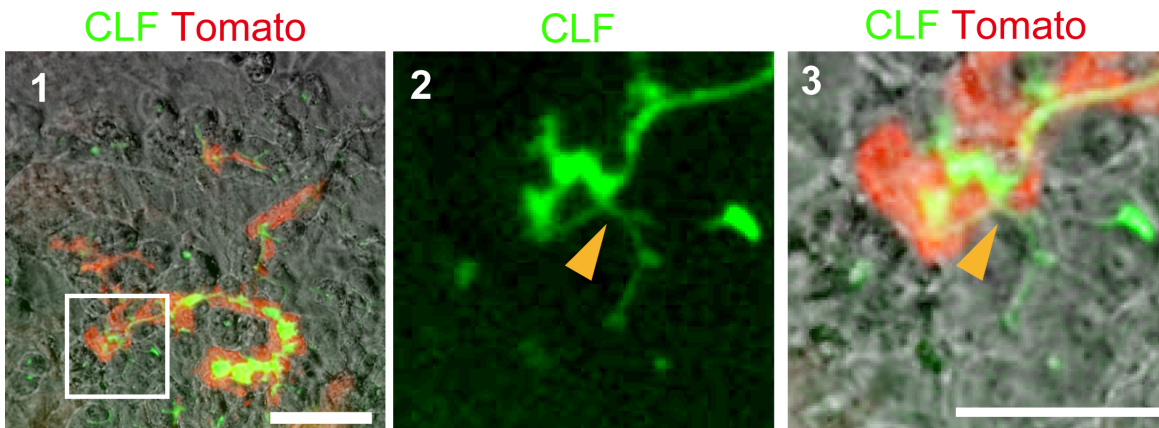


Figure 6

Human hepatocytes and mouse cholangiocytes form hybrid HBTO. A. hCLiP form bile canaliculi in co-culture with cholangiocytes. Bile canaliculi formed in co-culture are indicated by arrowheads (panel 4). hCLiP and mouse Tomato+ cholangiocytes were co-cultured to induce human-mouse hybrid HBTOs. Boxes in panels 1 and 3 are enlarged in panels 2 and panels 4. Bars represent 100 μ m B. Hepatobiliary junction in a hybrid HBTO. The bile canaliculi in an HNF4 α + hepatocyte cluster (line a in panel 1, and

panels a-1&a-2) is connected to the lumen of a Tomato+ mouse biliary structure (line c in panel 1, and panels c-1&c-2) via the luminal structure surrounded by HNF4 α + hepatocyte and Tomato+ mouse cholangiocytes (line b in panel 1, and panels b-1&b-2). Bars represent 20 μ m. C. Hybrid HBTOs take up CLF and transport it to the biliary tissue. CLF taken up by hCLiP is transported to the biliary tissue consisting of mouse cholangiocytes. The hepatobiliary connection is indicated by arrowheads (panels 2&3). The box in panel 1 is enlarged in panels 2 and 3. Bars in panels 1 and 3 are 200 and 50 μ m, respectively.

Supplementary Files

This is a list of supplementary files associated with this preprint. Click to download.

- [SupFigs201021.pdf](#)
- [SupFigs201021.pdf](#)
- [nrreportingsummaryNT.pdf](#)